DSP-Free Carrier Phase Recovery System for Laser-Forwarded Offset-QAM Coherent Optical Receivers

Marziyeh Rezaei, Daniel Sturm, Pengyu Zeng, and Sajjad Moazeni*

Department of Electrical and Computer Engineering

University of Washington

Seattle, USA

*smoazeni@uw.edu

Abstract—Co-packaged optics (CPO) are emerging as a promising solution to address future off-package I/O bandwidth scalability challenges. While previously proposed CPO solutions have primarily focused on pulse amplitude modulation (PAM), employing coherent modulation techniques could further enhance data rates. However, optical coherent transceivers often exhibit high power consumption and inefficient use of area. In this work, we propose a new DSP-free carrier phase recovery system for offset-QAM modulation based on a laser-forwarding technique. Offset-QAM can be realized with lower area and power optical modulators. The proposed approach is simulated and validated using Global Foundry monolithic 45nm silicon photonics PDK models with the circuit/system-level implementation at 25GBaud offset-QAM-4. This technique can also be extended to higher-order modulations such as QAM-16.

Index Terms—Optical interconnects, Optical receiver, Offset-QAM, Carrier phase recovery, Costas loop.

I. INTRODUCTION

As AI/ML accelerators, GPUs, and network switches increasingly demand tens of Tb/s of off-package IO bandwidth, the adoption of co-packaged optics (CPO) is becoming inevitable [1]. Wavelength and polarization division multiplexing (WDM/PDM) have been proposed for CPO to enhance data rates per fiber [2]. However, these techniques can offer only limited scalability due to practical constraints (e.g., limited available laser lines for WDM). Therefore, achieving energyefficient higher data rates will necessitate more advanced and coherent modulations. Currently, CPO utilizes only amplitude modulation, such as pulse amplitude modulation (PAM) (e.g., NRZ and PAM-4). Increasing data rates with the current amplitude modulation is unfeasible because the electronic control and driving circuitry would consume immense power and have higher noise at higher bandwidths. Coherent modulations bring advantages, such as higher receiver gain and noise suppression. While coherent optics using quadrature amplitude modulation (QAM) have been widely employed for long-haul (+10km) applications with Mach Zehnder Modulator (MZM)based transmitters [3], the large footprint of these devices (multi- mm^2) and requirements for large voltage swings make them impractical for meeting the necessary shoreline and aerial bandwidth densities for CPO [4]. Moreover, today's coherent links rely on power-hungry DSPs for signal processing, including carrier (or laser) frequency/phase recovery [5], which is not affordable within sub-pJ/b ideal energy goals for CPO for inter/intra-rack communications [6].

To enable energy- and area-efficient QAM modulation, offset-QAM can be employed. This type of optical modulation can be generated by using a fraction of π phase-shift rather than a full- π , which is typically needed in QAM-4 (QPSK). This allows for shorter MZMs with partial voltage drive swings [7]. While this leads to lower optical modulation amplitude (OMA), it provides an extra dimension beyond wavelength/polarization for increasing the data rate.

While many functionalities of today's DSPs in coherent links are unnecessary in inter/intra-rack links [8], laser phase recovery is required. Coherent optical communication relies on the precise phase/frequency alignment of the receiver (Rx) signal and local oscillator (LO) at the receiver. DSP-free methods such as the Costas loop method have been demonstrated for laser phase and frequency recovery in conventional QAM-4 (QPSK) systems [9]. The phase error signal generated by a Costas loop can be used in conjunction with various loop architectures to either directly control the local laser phase/frequency and/or tune the phase of the LO signal using an electro-optical or thermal phase shifter [3], [10]–[12].

However, the aforementioned techniques cannot be directly applied to offset-QAM since the signal constellation is not centered around the origin. In this work, we propose a new method for DSP-free carrier phase recovery systems for offset-QAM modulation. In this method, we detect the phase offset between the Rx and LO paths based on the average power/voltage difference between the in-phase (I) and quadrature (Q) signals, which is proportional to the phase offset $(\Delta \phi)$. This difference is then used as an error signal to compensate for the phase error by using a phase shifter in the LO path for laser-forwarded links [13]. Laser-forwarded coherent links are a promising approach to avoid using another laser at the receiver for 100mrange links. In doing so, the receiver only needs to perform phase recovery. We have implemented and simulated the proposed design using the Global Foundry 45SPCLO photonic and CMOS spectre models in Cadence. Such a simulation

framework and modeling are crucial for designing electronicphotonic systems, particularly precise closed-loop circuits.

The paper is organized as follows: Section II elaborates on offset-QAM modulation and various phase error detection techniques. The proposed approach and design implementation are described in Section III. Section IV presents the simulation results, and finally, we conclude the paper in Section V.

II. LASER-FORWARDED OFFSET-QAM CARRIER PHASE RECOVERY SYSTEM

Optical coherent communication relies on the precise frequency and phase locking/tracking of the received signal and the local oscillator (e.g., laser). Any phase error between the two paths $(\Delta \phi)$ causes I/Q cross-talk and reduces the detected signal power at the receiver, significantly degrading the Bit/Symbol Error Rates (SER and BER). Fig. 1 shows the constellation diagrams for conventional QAM-4 (QPSK) and offset-QAM-4, illustrating the effect of phase offset between the Rx and LO signals. In QAM-4 (QPSK), a $\Delta \phi$ phase offset causes the entire constellation to rotate around the origin and the Costas loop technique [11], [12] is utilized to calculate $\Delta \phi$. However, in the case of offset-QAM, the rotation not only affects amplitudes but also shifts the center of the constellation, making the conventional Costas loop ineffective. In this work, we propose a phase error detection technique based on measuring the average amplitude of I/Q symbols for offset-QAM carrier phase recovery systems.

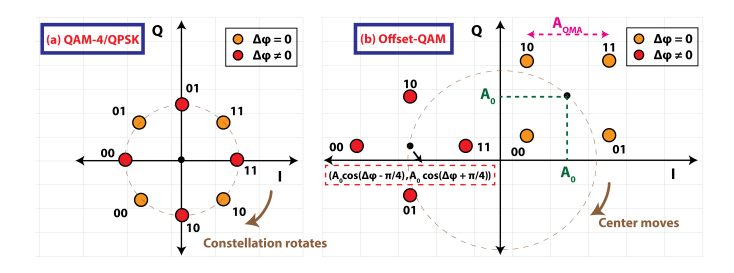


Fig. 1. The constellation of (a) QAM-4 (QPSK) (b) offset-QAM modulation with and without the phase error between the Rx and LO paths.

Fig. 2 illustrates the proposed architecture for correcting and aligning the phase of the Rx signal and LO signal using a tunable phase shifter in the LO path. To detect the phase error between the Rx and LO signals, two techniques can be deployed, as shown in Fig. 3. The I and Q signals before any phase error compensation are described by the following equations:

$$I'(t) = (I(t) + A_0)cos(\Delta\phi) + (Q(t) + A_0)sin(\Delta\phi)$$

$$Q'(t) = (Q(t) + A_0)cos(\Delta\phi) - (I(t) + A_0)sin(\Delta\phi)$$
 (1)

where A_0 is a constant value due to offset-QAM modulation and I(t)/Q(t) are $\pm A_{OMA}/2$. The high-frequency portions

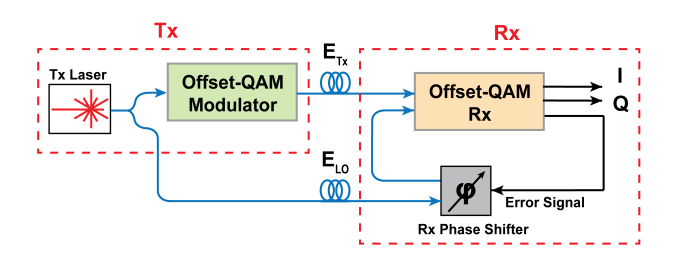


Fig. 2. Laser-forwarded offset-QAM coherent link with carrier (laser) phase recovery.

of I'(t) and Q'(t) are filtered using low-pass filters, retaining the average voltage of the signal as shown below:

$$I_{avg} = A_0 cos(\Delta \phi) + A_0 sin(\Delta \phi)$$

$$Q_{avg} = A_0 cos(\Delta \phi) - A_0 sin(\Delta \phi)$$
(2)

In Method 1, the outputs of the low-pass filters in the I and Q paths are subtracted, generating an error signal equal to $2A_0 \times \sin{(\Delta\phi)}$ as depicted in Fig. 4. However, if the error signal is in the region where the slope of the error signal has a positive sign, the loop will have a positive feedback and become unstable. To ensure loop stability, we use the negative slope of the error signal. For this purpose, we use the summation of I_{avg} and Q_{avg} $(2A_0 \times \cos{(\Delta\phi)})$ as a select signal to choose between $2A_0 \times \sin{(\Delta\phi)}$ and $2A_0 \times \sin{(\Delta\phi)}$. As a result, the error signal will be equal to $2A_0 \times \sin{(\Delta\phi)}$ for $n\pi/2 < \Delta\phi < (n+2)\pi/2$ as shown in Fig. 4. In Method 2, I_{avg} and Q_{avg} are sent to the limiting amplifiers (SGN) and mixers, and then subtracted, similar to the Costas loop technique generating an error signal equal to $\sqrt{2}A_0/2 \times \sin{(\Delta\phi)}$ for $n\pi/4 < \Delta\phi < (n+2)\pi/4$ [11], [12].

As depicted in Fig. 4, Method 2 produces a sawtooth error signal that provides constant gain over the entire range. However, this error signal has a periodicity of $\pi/2$, with zero values at $\pm n\pi/2$ and $\pm n\pi$, causing 90° phase ambiguity between the I and Q signals at the receiver [11]. To overcome this issue, preliminary differential coding during transmission and differential decoding after demodulation have been proposed [14]. On the other hand, Method 1 does not suffer from 90° phase ambiguity issues; however, the gain starts to drop near the peaks and troughs, affecting loop metrics such as loop bandwidth and locking time (phase compensation time). In this work, we employ the phase detection technique based on Method 1.

III. CADENCE IMPLEMENTATION OF THE PROPOSED DESIGN

Fig. 5 illustrates the block diagram of the proposed receiver. The laser output is divided into two paths. The transmitter generates an offset-QAM signal using I and Q data from PRBS generators. The optical transmitter is implemented using amplitude modulators and thermal phase shifters. The modulated signal, along with the LO signal, is transmitted to the receiver through fibers. At the receiver, the received signal beats with

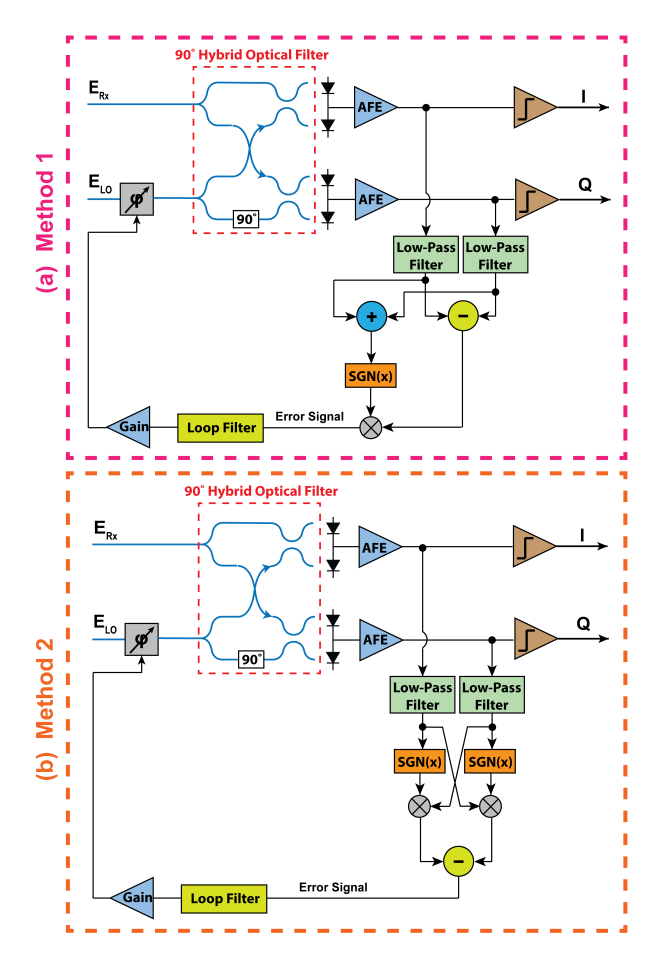


Fig. 3. Block diagrams of the proposed offset-QAM coherent receiver using (a) Method 1 and (b) Method 2 for laser phase recovery.

the LO signal in a 90° optical hybrid filter to demodulate I and Q signals. Balanced photodetectors (PD) convert the optical signals into the electrical domain. The high-speed analog front end (AFE) comprises a trans-impedance amplifier (TIA) followed by a Continuous Time Linear Equalizer (CTLE). The subtractor, followed by a capacitor, generates the error signal proportional to $\sin(\Delta\phi)$. The adder, followed by a comparator, is used to select only the negative slope of the error signal to ensure stability. The opamp with capacitive feedback creates a second-order loop filter to guarantee zero remaining phase error between the LO and Rx signals. The driver continuously adjusts the phase shifter's phase in the LO path with the error signal (v_{err}) until the loop is locked and the I and Q averages become equal.

IV. SIMULATION RESULTS

We have designed and simulated our proposed laser-forwarded carrier phase recovery system in Cadence. Fig. 5 illustrates the parameter values used in this design. The baud rate is 25GBaud with a data rate of 50Gb/s for offset-QAM-4. To properly filter the data while achieving sufficient phase margin, the open-loop bandwidth is set to 40MHz. The

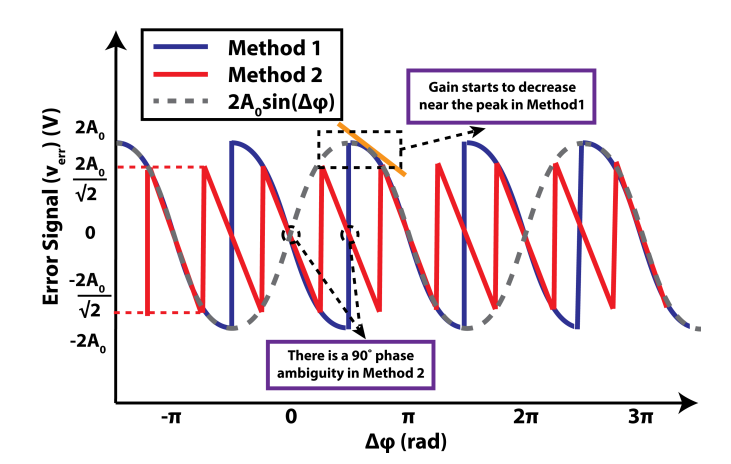


Fig. 4. The error signal generated by Method 1 and Method 2.

linearized open-loop transfer function of the design is shown below:

$$H_{\text{Open-Loop}}(s) = \frac{K_{\text{PD}} \times K_{\text{PS}} \times e^{-s\tau} \times (1 + \frac{s}{w_{\text{LF}}})}{s \times (1 + \frac{s}{w_{\text{PS}}})}$$

$$K_{\text{PD}} = \frac{4\sqrt{2}}{\pi} I_0 \times K_{\text{AFE}} \times K_{\text{LF}} \times K_{\text{driver}} \ (V/rad)$$

$$I_0 = |\overline{E_{I/Q}}| \times |E_{LQ}| \times R_{PD}$$
 (3)

where w_{PS} specifies the 3-dB bandwidths of the phase shifter (PS), w_{LF} is the loop filter's (LF) zero, and τ is the optical delay presented to the loop, which is negligible due to low loop bandwidth. I_0 is the I/Q signal's average photocurrent at the output of the balanced PDs. $|E_{LO}|$ and $|\overline{E_{I/Q}}|$ are the E-field magnitudes of the LO signal and the average of the I and Q signals, respectively. $|\overline{E_{I/Q}}|$ is equal to A_0 for DCbalanced I/Q data streams. R_{PD} represents the photodiode responsivity. K_{AFE} , K_{LF} , and K_{driver} are the gain of the AFE, loop filter, and phase shifter driver, respectively. K_{PS} is the linearized voltage-to-phase conversion gain of the phase shifter. It is noteworthy that for Method 1, K_{PD} is not constant and shows variation near the peak; however, for simplicity, K_{PD} is approximated by its value in the linear region. It is worth mentioning that Method 2 follows the same open-loop transfer function as Method 1 (the gain of the mixer should be added to K_{PD}).

The thermal phase shifter has a bandwidth of approximately 2kHz. To achieve a phase margin of 72.5° , a total gain of 10^{10} ($K_{PD} \times K_{PS}$) with $w_{LF} = 318kHz$ is required. I_0 is chosen based on the sensitivity of the receiver and the power of the Tx laser, which is beyond the scope of this paper. v_{err} provides a swing range of 250mV to 1.8V that can compensate for approximately 5π phase offset between the Rx and LO signals.

To evaluate the functionality of the design, we performed the closed-loop simulation for $\Delta\phi=\pi/3$ and $\Delta\phi=2\pi/3$. Fig. 6 (a) shows the error signal and the phase of the LO signal. As shown in this figure, the loop locks at around 5μ s with a phase variation of less than 0.2° . Note that the sharp transition in

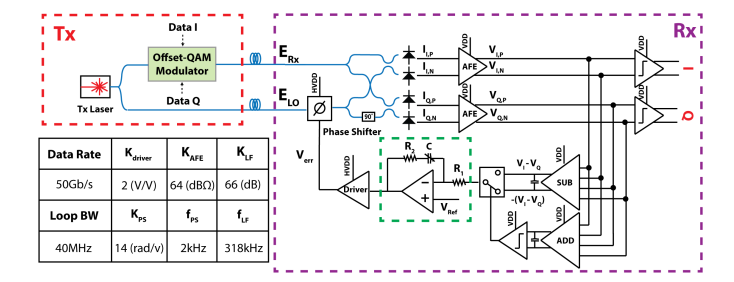


Fig. 5. Design parameters and the circuit-level block diagram of the proposed carrier phase recovery system.

the graph is due to phase-wrapping of the phase shifter. Fig. 6 (b) shows the eye diagram of the I and Q signals at the input of the AFE when the loop is locked. Fig. 6 (c) shows the I and Q eye diagram when the phase error is compensated using open-loop tuning. As can be seen, the vertical and horizontal eye-openings in the closed-loop results almost match the open-loop compensation. It is worth mentioning that the simulation results of Method 1 and Method 2 match for $\Delta \phi = \pi/3$ and $2\pi/3$.

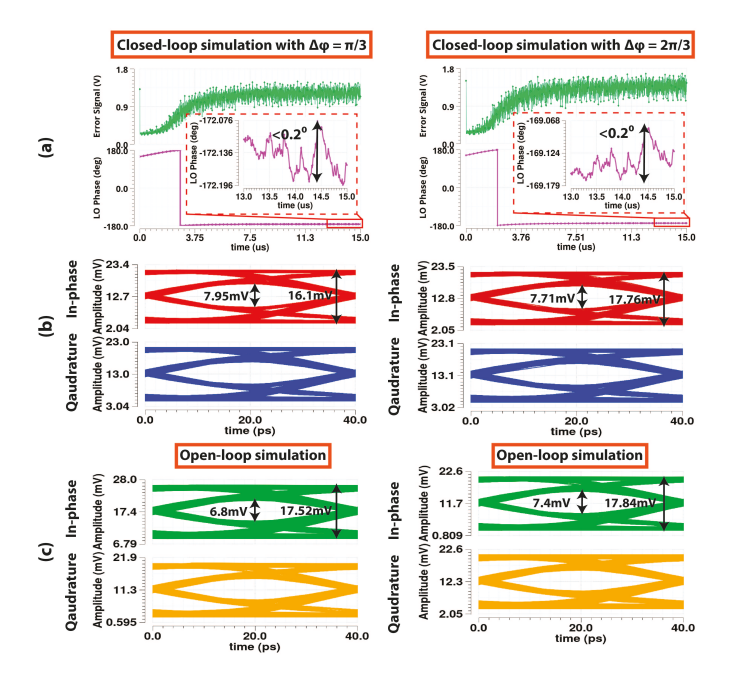


Fig. 6. System results for the offset-QAM receiver with a phase offset of $\pi/3$ and $2\pi/3$ at 25GBaud: (a) voltage error signal (v_{err}) and phase error, (b) I/Q eye diagrams with the proposed closed-loop phase recovery technique, (c) the open-loop compensation.

V. CONCLUSION

We have proposed and evaluated a DSP-free laser-forwarded carrier phase recovery system for offset-QAM modulation. Offset-QAM enables a power/area-efficient optical I/O method for both inter- and intra-rack communication at high data rates. The proposed technique can be implemented with minimal circuit area/power overhead, eliminating the need for an additional local oscillator (laser) at the receiver. The design has been verified and simulated in Cadence using the GF 45nm

monolithic silicon photonics process at a 25GBaud QAM-4 receiver. Our approach is adaptable for higher-order QAM modulations and baud rates as well.

ACKNOWLEDGMENT

This work is supported by NSF CAREER (ECCS-2142996). The authors would like to thank GlobalFoundries for providing silicon fabrication and PDK through the 45SP-CLO university program.

REFERENCES

- M. et al., "Co-packaged photonics for high performance computing: Status, challenges and opportunities," *Journal of Lightwave Technology*, vol. 40, no. 2, pp. 379–392, 2022.
- [2] P. J. Winzer, "The future of communications is massively parallel," J. Opt. Commun. Netw., vol. 15, no. 10, pp. 783–787, oct 2023. [Online]. Available: https://opg.optica.org/jocn/abstract.cfm?URI=jocn-15-10-783
- [3] L. A. Valenzuela, Y. Xia, A. Maharry, H. Andrade, C. L. Schow, and J. F. Buckwalter, "A 50-GBaud QPSK optical receiver with a phase/frequency detector for energy-efficient intra-data center interconnects," *IEEE Open Journal of the Solid-State Circuits Society*, vol. 2, pp. 50–60, 2022.
- [4] J. He, Y. Zhang, H. Liu, Q. Liao, Z. Zhang, M. Li, F. Jiang, J. Shi, J. Liu, N. Wu et al., "A 56-gb/s reconfigurable silicon-photonics transmitter using high-swing distributed driver and 2-tap in-segment feed-forward equalizer in 65-nm cmos," *IEEE Transactions on Circuits and Systems I: Regular Papers*, vol. 69, no. 3, pp. 1159–1170, 2021.
- [5] T. Kobayashi, J. Cho, M. Lamponi, G. De Valicourt, and C. R. Doerr, "Coherent Optical Transceivers Scaling and Integration Challenges," Proceedings of the IEEE, vol. 110, no. 11, pp. 1679–1698, 2022.
- [6] S. Moazeni, "Next-generation Co-Packaged Optics for Future Disaggregated AI Systems," in OCP Future Technologies Symposium, 2022.
- [7] G.-W. Lu, M. Sköld, P. Johannisson, J. Zhao, M. Sjödin, H. Sunnerud, M. Westlund, A. Ellis, and P. A. Andrekson, "40-Gbaud 16-QAM transmitter using tandem IQ modulators with binary driving electronic signals," *Opt. Express*, vol. 18, no. 22, pp. 23 062–23 069, oct 2010. [Online]. Available: https://opg.optica.org/oe/abstract.cfm?URI=oe-18-22-23062
- [8] A. A. M. Saleh, K. E. Schmidtke, R. J. Stone, J. F. Buckwalter, L. A. Coldren, and C. L. Schow, "INTREPID program: technology and architecture for next-generation, energy-efficient, hyper-scale data centers," J. Opt. Commun. Netw., vol. 13, no. 12, pp. 347–359, dec 2021. [Online]. Available: https://opg.optica.org/jocn/abstract.cfm? URI=jocn-13-12-347
- [9] H.-c. Park, M. Lu, E. Bloch, T. Reed, Z. Griffith, L. Johansson, L. Coldren, and M. Rodwell, "40Gbit/s coherent optical receiver using a Costas loop," *Opt. Express*, vol. 20, no. 26, pp. B197—B203, dec 2012. [Online]. Available: https://opg.optica.org/oe/abstract.cfm?URI= oe-20-26-B197
- [10] R. Ashok, N. Nambath, and S. Gupta, "Carrier phase recovery and compensation in analog signal processing based coherent receivers," *Journal of Lightwave Technology*, vol. 40, no. 8, pp. 2341–2347, 2021.
- [11] R. Ashok, S. Naaz, R. Kamran, and S. Gupta, "Analog domain carrier phase synchronization in coherent homodyne data center interconnects," *Journal of Lightwave Technology*, vol. 39, no. 19, pp. 6204–6214, 2021.
- [12] G. Movaghar, V. Arrunategui, J. Liu, A. Maharry, C. Schow, and J. Buckwalter, "A 112-Gbps, 0.73-pJ/bit Fully-Integrated O-band IQ Optical Receiver in a 45-nm CMOS SOI-Photonic Process," in 2023 IEEE Radio Frequency Integrated Circuits Symposium (RFIC). IEEE, 2023, pp. 5–8.
- [13] N. Mehta, S. Lin, B. Yin, S. Moazeni, and V. Stojanović, "A Laser-Forwarded Coherent Transceiver in 45-nm SOI CMOS Using Monolithic Microring Resonators," *IEEE Journal of Solid-State Circuits*, vol. 55, no. 4, pp. 1096–1107, 2020.
- [14] B. Shakhtarin, V. Sizykh, and A. Sidorkina Yu, "Sinkhronizatsiya v radiosvyazi i radionavigatsii [synchronization in radio communication and navigation]," Moscow, Goryachaya Liniya-Telekom Publ, 2011.